



available at www.sciencedirect.com



journal homepage: www.elsevier.com/locate/jhydrol



Two-dimensional modelling of preferential water flow and pesticide transport from a tile-drained field

Annemieke I. Gärdenäs^{a,*}, Jirka Šimůnek^b, Nicholas Jarvis^a,
M.Th. van Genuchten^c

^a Department of Soil Sciences, Swedish University of Agricultural Sciences, P.O. Box 7014, 750 07 Uppsala, Sweden

^b Department of Environmental Sciences, University of California, Riverside, 900 University Avenue, A135 Bourns Hall, Riverside, CA 92521, USA

^c George E. Brown, Jr. Salinity Laboratory, USDA-ARS, 450 West Big Springs Road, Riverside, CA 92507, USA

Received 6 April 2005; received in revised form 16 March 2006; accepted 20 March 2006

KEYWORDS

Preferential flow
and transport;
Dual-permeability;
Pesticide leaching;
Tile drainage;
HYDRUS-2D

Summary Preferential flow through soil macropores in tile drained soils can significantly increase the risk of pollution of surface water bodies by agricultural chemicals such as pesticides. While many field studies have shown the importance of preferential flow in tile-drained fields, few have included detailed numerical modelling of the processes involved. The objective of this study was to compare four conceptually different preferential flow and/or transport approaches for their ability to simulate drainage and pesticide leaching to tile drains. The different approaches included an equilibrium approach using modified hydraulic properties near saturation, and three non-equilibrium approaches: a mobile–immobile solute transport model, a dual-porosity approach, and a dual-permeability formulation. They were implemented into the HYDRUS-2D software package. The model predictions were compared against measurements of drainage and pesticide concentrations made at an undulating, tile-drained field in southern Sweden (Näsbygård) during a period of 6 weeks following spray application of the herbicide MCPA.

The dual-permeability approach most accurately simulated preferential drainage flow, even though this approach somewhat overestimated the drainage rates. The equilibrium and mobile–immobile approaches largely failed to capture the preferential flow process. The dual-porosity approach predicted much more distinct and higher drainage flow events as compared to the dual-permeability approach. Differences between measured and simulated tile drainage

* Corresponding author. Tel.: +46 18 672294; fax: +46 18 672795.

E-mail addresses: Annemieke.Gardenas@mv.slu.se (A.I. Gärdenäs), Jiri.Simunek@ucr.edu (J. Šimůnek), Nicholas.Jarvis@mv.slu.se (N. Jarvis), rvang@ussl.ars.usda.gov (M.Th. van Genuchten).

rates using the dual-permeability approach could be partly explained by water by-passing the tile drains and recharging the deeper aquifer. The dual-permeability and dual-porosity approaches closely captured the dynamics in measured pesticide concentrations. Both the equilibrium and mobile–immobile approaches completely failed to match measured MCPA leaching by underestimating the peak concentrations by more than two orders of magnitude. We conclude that two-dimensional models are suitable tools for studying pesticide leaching from undulating fields with large spatial variability in soil properties.

© 2006 Elsevier B.V. All rights reserved.

Introduction

Rapid non-equilibrium flow through soil macropores is a widespread phenomenon that can profoundly affect solute transport into and through the unsaturated zone. The resulting preferential flow process can dramatically increase the risk of groundwater pollution by surface-applied chemicals (e.g., see reviews by Flury, 1996; and Jarvis, 2002). The importance of macropore flow for solute transport has been demonstrated repeatedly by means of breakthrough experiments on small, undisturbed soil columns. Results of such experiments have often been interpreted in terms of one-dimensional dual-porosity and dual-permeability models appropriate to that scale (e.g. Saxena et al., 1994; Brown et al., 1999; Castiglione et al., 2003; Köhne et al., 2004; Pot et al., 2005). However, quantitative information about the significance of non-equilibrium processes for solute transport at the field-scale is still very much lacking. Replicated breakthrough experiments have shown large variations in transport behaviour between individual columns, ranging from rapid breakthrough due to macropore flow, to essentially zero leaching (e.g. Jarvis et al., 1994; Lennartz, 1999). This may cause difficulties in upscaling from the column to the field scale in a one-dimensional framework, since effective macropore flow parameters are often poorly identifiable (e.g., Czapar et al., 1992; Kamra et al., 2001; Akhtar et al., 2003).

Two- and three-dimensional modelling approaches should be more appropriate for field situations, where large within-field spatial variations in soil properties occur and where differences in topography can lead to significant lateral flow along hillslopes. For example, Christiansen et al. (2004) showed in a recent study of flow and transport at the catchment scale, that the degree of preferential flow significantly varied with topography and depth to groundwater within the catchment.

Preferential flow and transport can be especially important in macroporous field soils that are also tile drained, thus significantly increasing the risk of pollution of nearby surface water by agricultural chemicals such as pesticides or nutrients (Stamm, 1997; Kohler et al., 2001). While many field studies have shown the importance of preferential flow in tile-drained fields, few have included detailed numerical modelling of the processes involved (Abbaspour et al., 2001; Kohler et al., 2003; Köhne and Gerke, 2005).

The objective of this study was to compare various preferential flow and/or transport models in terms of their ability to simulate the measured dynamics of water drainage and pesticide leaching from an undulating, tile-drained agricultural field in Southern Sweden. Four different and com-

monly-used conceptual approaches were implemented in the HYDRUS-2D two-dimensional transport model (Šimůnek et al., 1999, 2003): (a) an equilibrium approach using soil hydraulic properties modified close to saturation to account for accelerated flow (Vogel and Císlerová, 1988), and three non-equilibrium approaches involving (b) the mobile–immobile water concept for non-equilibrium transport combined with standard equilibrium water flow (van Genuchten and Wierenga, 1976), (c) a dual-porosity approach for both water flow and solute transport (Šimůnek et al., 2003), and (d) a dual-permeability formulation assuming non-equilibrium flow and transport in both domains (Gerke and van Genuchten, 1993a, 1996).

Theory

The modified version of HYDRUS-2D (Šimůnek et al., 1999, 2003) includes one equilibrium approach for using modified hydraulic properties near saturation, and three non-equilibrium approaches i.e., the mobile–immobile water, dual-porosity and dual-permeability approaches. They have in common that water flow is simulated using the Richards equation and solute transport using the convection-dispersion equation. The modelling approaches differ in terms of (a) the division of the pore space between matrix and macropore domains, (b) in which part of the porous medium (i.e., the matrix and/or macropore domain) water flow and solute transport take place, and (c) the definition of mass transfer, if present, between the two pore domains (Table 1). For example, since the equilibrium approach assumes a single-pore system, this model is strictly not a preferential flow model in that the approach still predicts uniform flow and transport. The dual-porosity approach assumes that water flow and transport are restricted only to the macropore domain, but with possible exchange of water and solute between the macropore and matrix

Table 1 Pore regions that are active for water flow and solute transport using the different modeling approaches

Approach	Water flow		Solute transport	
	Matrix	Macropore	Matrix	Macropore
Equilibrium	+		+	
Mobile–immobile	+			+
Dual-porosity		+		+
Dual-permeability	+	+	+	+

domains. Detailed descriptions of the various modelling approaches are given below separately for water flow and solute transport.

Water flow

Equilibrium approach with modified hydraulic properties
Variably-saturated flow is calculated using the Richards equation:

$$\frac{\partial \theta}{\partial t} = \frac{\partial}{\partial x_i} \left(K_{ij} \frac{\partial h}{\partial x_j} + K_{iz} \right) - S \quad (1)$$

where θ is the volumetric water content (L^3L^{-3}), h is the pressure head (L), S is a sink term (T^{-1}), x_i ($i = 1, 2$) are the spatial coordinates (L), t is time (T), and K_{ij} are components of the unsaturated hydraulic conductivity tensor (LT^{-1}). We assumed the soil in each layer to be isotropic, with both entries, K_{xx} and K_{zz} , equal to the unsaturated hydraulic conductivity function, $K(h)$. The van Genuchten–Mualem model (van Genuchten, 1980) was used to characterize the unsaturated soil hydraulic properties

$$\theta(h) = \theta_r + \frac{\theta_s - \theta_r}{\left[1 + |\alpha h|^n\right]^m} \quad (2)$$

$$K(h) = K_s K_r(h) = K_s S_e^l \left[1 - \left(1 - S_e^{1/m}\right)^m\right]^2 \quad (3)$$

where θ_r and θ_s denote the residual and saturated water contents (L^3L^{-3}), respectively; K_s (LT^{-1}) and $K_r(-)$ are the saturated and relative hydraulic conductivities, respectively; α is related to the inverse of a characteristic pore radius (L^{-1}), n is a pore-size distribution index ($-$), l is a pore-connectivity parameter ($-$), and $m = 1 - 1/n$ ($-$).

The effect of macropores on variably-saturated water flow is often described using composite functions such as those suggested by Durner (1994) and Mohanty et al. (1997), among others. In this study, we use the composite model suggested by Vogel and Císlarová (1988). The approach assumes that capillary-dominated flow can be described using Eq. (3) for the unsaturated hydraulic conductivity at pressure heads less than a critical pressure head, h_k , while a linear increase in conductivity is assumed between h_k and saturation to account for non-capillary, macropore dominated flow, i.e.:

$$K(h) = \begin{cases} K_s K_r(h) & h \leq h_k \\ K_k - \frac{h-h_k}{h_k} (K_s - K_k) & h_k < h < 0 \\ K_s & h \geq 0 \end{cases} \quad (4)$$

where K_k is the hydraulic conductivity at h_k .

Dual-porosity approach

Dual-porosity models assume that water flow is restricted to the macropore or fracture domain (the inter-aggregate pore domain) and that water in the matrix (the intra-aggregate pore domain) does not move at all (van Genuchten and Wierenga, 1976; Šimůnek et al., 2003). The approach assumes that the liquid phase can be partitioned into mobile (flowing), θ_f , and immobile (stagnant), θ_m , regions such that the total water content is given by

$$\theta = \theta_f + \theta_m \quad (5)$$

while water and/or solutes are allowed to exchange between the two regions. We will use here the subscript f for the fracture or macropore region and m for the soil matrix.

The dual-porosity formulation as used here for variably-saturated flow employs the Richards Eq. (1) to describe flow in the macropores, and a mass balance equation to describe moisture dynamics in the matrix as follows (Šimůnek et al., 2003):

$$\frac{\partial \theta_f}{\partial t} = \frac{\partial}{\partial x_j} \left[K_{ij} \left(\frac{\partial h}{\partial x_j} + K_{iz} \right) \right] - S_f - \Gamma_w \quad (6)$$

$$\frac{\partial \theta_m}{\partial t} = -S_m + \Gamma_w$$

where S_f and S_m are sink terms for both regions (T^{-1}), and Γ_w is the transfer rate for water from the inter- to the intra-aggregate pores (T^{-1}). The water mass transfer rate in (6) is assumed to be proportional to the difference in the pressure head between the macropore and matrix regions (Gerke and van Genuchten, 1993b):

$$\Gamma_w = \alpha_w (h_f - h_m) \quad (7)$$

in which α_w is a first-order mass transfer coefficient ($L^{-1}T^{-1}$):

$$\alpha_w = \frac{\beta}{d^2} K_a(h) \gamma_w \quad (8)$$

where d is an effective diffusion path-length (i.e. half the aggregate width) (L), β is a shape factor that depends on the geometry of the soil aggregates ($-$), γ_w is a scaling factor ($-$) (Gerke and van Genuchten, 1993b), and K_a is the effective hydraulic conductivity of the fracture–matrix interface (LT^{-1}) determined as a simple arithmetic average involving both h_f and h_m as follows:

$$K_a(h) = 0.5[K_a(h_m) + K_a(h_f)] \quad (9)$$

Dual-permeability approach

Dual-permeability approaches assume that water flow and solute transport can take place in both the macropores and the matrix. Some models invoke similar equations for flow in both regions, while others use different formulations (e.g. as in Larsbo and Jarvis, 2003). In this study we use the approach of Gerke and van Genuchten (1993a, 1996) who applied the Richards equation to both pore regions. The flow equations for the macropore (subscript f) and matrix (subscript m) pore systems are then given by:

$$\frac{\partial \theta_f}{\partial t} = \frac{\partial}{\partial x_j} \left(K_{ij}^f \frac{\partial h_f}{\partial x_j} + K_{iz}^f \right) - S_f - \frac{\Gamma_w}{w} \quad (10)$$

$$\frac{\partial \theta_m}{\partial t} = \frac{\partial}{\partial x_j} \left(K_{ij}^m \frac{\partial h_m}{\partial x_j} + K_{iz}^m \right) - S_m + \frac{\Gamma_w}{1-w} \quad (11)$$

where w is the ratio of the volume of the macropore domain to the total soil volume. Following Gerke and van Genuchten (1993a), the mass transfer term in the dual-permeability approach is given by Eqs. (7)–(9). Note that the water contents θ_f and θ_m in (10) and (11) have different meanings than in (6) where they represented water contents of the total pore space (i.e., $\theta = \theta_f + \theta_m$), while they refer here to water contents of the two separate (fracture or matrix) pore domains such that $\theta = w\theta_f + (1-w)\theta_m$.

Solute transport

Equilibrium approach

Solute transport in the physical equilibrium approach is described using the convection-dispersion equation given by:

$$\frac{\partial \theta c}{\partial t} + \frac{\partial \rho s}{\partial t} = \frac{\partial}{\partial x_i} \left(\theta D_{ij} \frac{\partial c}{\partial x_j} \right) - \frac{\partial q_i c}{\partial x_i} - \phi \quad (12)$$

where c (ML^{-3}) and s (MM^{-1}) are solute concentrations in the liquid and solid phases, respectively, q_i is the vector for the volumetric water flux density (LT^{-1}), ρ is the soil bulk density (ML^{-3}), and D_{ij} is the dispersion tensor (L^2T^{-1}). In this study, the decay term, ϕ ($\text{ML}^{-3}\text{T}^{-1}$), represents the effects of first-order degradation of MCPA as controlled by the rate constants μ_w and μ_s for the liquid and solid phases, respectively.

Mobile–immobile water

The HYDRUS -2D code (Šimůnek et al., 1999) allows the concepts of mobile and immobile water to be used for solute transport in combination with equilibrium water flow. As for the dual-porosity formulation, this approach assumes that the liquid phase can be partitioned into mobile, θ_f , and immobile, θ_m , regions, with convective-dispersive transport being restricted to only the mobile region:

$$\begin{aligned} \frac{\partial \theta_f c_f}{\partial t} + \frac{\partial f \rho s_f}{\partial t} &= \frac{\partial}{\partial x_i} \left(\theta_f D_{ij}^f \frac{\partial c_f}{\partial x_j} \right) - \frac{\partial q_i c_f}{\partial x_i} - \phi_f - \Gamma_s \\ \frac{\partial \theta_m c_m}{\partial t} + \frac{\partial (1-f) \rho s_m}{\partial t} &= -\phi_m + \Gamma_s \end{aligned} \quad (13)$$

where c_f and c_m are the liquid concentrations in the macropore (mobile water) and matrix (immobile water) regions (ML^{-3}), respectively; s_f and s_m are the adsorbed concentrations in the mobile and immobile regions (MM^{-1}), respectively, f is the dimensionless fraction of sorption sites in contact with mobile water ($-$), D_{ij}^f is the dispersion tensor in the mobile region (L^2T^{-1}), ϕ_f and ϕ_m are reactions in the mobile and immobile regions ($\text{ML}^{-3}\text{T}^{-1}$), respectively, and Γ_s is the solute transfer rate between the two regions ($\text{ML}^{-3}\text{T}^{-1}$). This transfer rate is assumed to be proportional to the difference in concentration between the two regions:

$$\Gamma_s = \omega_s (c_f - c_m) \quad (14)$$

where $\omega_s (= \theta_{im} \alpha_s)$ is a rate coefficient containing both the immobile water content (L^3L^{-3}) and the mass-transfer coefficient α_s (T^{-1}). The above mobile–immobile water solute transport model assumes that the immobile water content is constant during the simulations.

Dual-porosity approach

Solute transport in a dual-porosity system can be described using the same governing equations as for the mobile–immobile water approach, except that the mass transfer term now also considers convective solute transfer with water moving between the two regions, in addition to diffusive mass transfer resulting from concentration gradients:

$$\Gamma_s = \omega_s (c_f - c_m) + \Gamma_w c^* \quad (15)$$

where c^* is equal to c_f for $\Gamma_w > 0$ and c_m for $\Gamma_w < 0$.

Dual-permeability approach

The dual-permeability approach assumes that convective-dispersive transport can occur in both the macropore and matrix domains:

$$\frac{\partial \theta_f c_f}{\partial t} + \frac{\partial \rho s_f}{\partial t} = \frac{\partial}{\partial x_i} \left(\theta_f D_{ij}^f \frac{\partial c_f}{\partial x_j} \right) - \frac{\partial q_i^f c_f}{\partial x_i} - \phi_f - \frac{\Gamma_s}{w} \quad (16)$$

$$\frac{\partial \theta_m c_m}{\partial t} + \frac{\partial \rho s_m}{\partial t} = \frac{\partial}{\partial x_i} \left(\theta_m D_{ij}^m \frac{\partial c_m}{\partial x_j} \right) - \frac{\partial q_i^m c_m}{\partial x_i} - \phi_m - \frac{\Gamma_s}{1-w} \quad (17)$$

where D_{ij}^f and D_{ij}^m (L^2T^{-1}) are the dispersion tensors in the macropore and matrix regions, respectively, and q_i^f and q_i^m (LT^{-1}) are the Darcian flux densities in the macropore and matrix regions, respectively. The transfer rate, α_s , for solutes between the macropore and matrix regions ($\text{ML}^{-3}\text{T}^{-1}$) is the sum of diffusive and convective transport as follows (Gerke and van Genuchten, 1996):

$$\Gamma_s = \alpha_s (1 - w_f) \theta_m (c_f - c_m) + \Gamma_w c^* \quad (18)$$

where c^* is equal to c_f for $\Gamma_w > 0$ and c_m for $\Gamma_w < 0$, and α_s is a first-order solute mass transfer coefficient (T^{-1}) of the form

$$\alpha_s = \frac{\beta}{d^2} D_a \quad (19)$$

in which D_a is an effective diffusion coefficient (L^2T^{-1}), representing the diffusion properties of the macropore–matrix interface.

Boundary conditions

Atmospheric boundary conditions were applied to the soil surface using (a) prescribed fluxes of precipitation, potential transpiration and evaporation, (b) a prescribed zero head (saturation) during ponding, and/or (c) equilibrium between the soil surface water content and atmospheric water vapour when atmospheric evaporative demand could not be met by the soil. Zero fluxes were ascribed to the lateral and bottom boundaries. Drains were represented by equivalent nodal sinks in a regular (structured) finite element mesh using an adjusted hydraulic conductivity, K_{drain} (LT^{-1}) following Vimoke et al. (1963) and Fipps et al. (1986):

$$K_{\text{drain}} = K(h) C_d \quad (20)$$

where C_d is a correction factor ($-$) determined from the ratio of the effective drain diameter d_e (L) and the side length of the square formed by finite elements with the adjusted hydraulic conductivity (Fipps et al., 1986).

Material and methods

Study area and soil sampling

The Näsbygård site is located in the southern-most part of Sweden in the vicinity of the city of Ystad ($55^\circ 26' \text{N}$; $13^\circ 27' \text{E}$, Fig. 1). The climate is warm-temperate (Köppen classification; Liljequist, 1970) with a mean annual temperature of 7.2°C and an average annual precipitation rate of 662 mm. The 32-ha field is part of the Vemmenhög catchment (9 km^2), formed in a glacial till with Eutric Cambisols (FAO, 1988) being the dominant soil type. The topography is strongly undulating with height differences of up to 3.5 m within 50 m distances. Previous studies at this field

site (Jarvis et al., 2001; Roulier and Jarvis, 2003) showed that the various landscape elements (i.e., hilltop, mid-slope and hollows) differ greatly in texture, structure and soil organic matter content, and hence in terms of the risk for pesticide leaching, including the potential for preferential flow and transport. Jarvis et al. (2001) found considerable spatial variability in soil texture and organic C content, mostly as a function of landscape position, while Roulier and Jarvis (2003) found similar dependencies of various macropore characteristics on landscape position in column tracer breakthrough experiments calibrated against the MACRO dual-permeability model. The organic C content was found to be as high as 5% in the topsoil of the hollows, as compared to 1.2% and 1.4% in the topsoil of the hilltops and mid-slopes, respectively. Pesticide sorption hence should be more extensive in the hollows, thus locally reducing the risk of pesticide transport. The hilltops have somewhat higher clay contents (24%, 17.3%, and 19.8% on average for the topsoils of hilltop, slope and hollow positions, respectively), leading to lower saturated hydraulic conductivities of the matrix, a better developed structure, and hence more pronounced macropore flow (Roulier and Jarvis, 2003).

A 50-m transect, from a hollow to a hilltop, in the NW–SE direction, was selected to represent the entire field and to investigate short-distance spatial variations in soil texture and organic matter content (Fig. 1). Soil texture and organic matter were sampled every two meters at 10–15, 35–40, 60–65 and 85–90 cm depth. The soil organic matter content was analyzed by loss on ignition at 550–600 °C during 3 h.

Soil texture (<2 mm) was analyzed by wet-sieving and sedimentation using the pipette method (Ljung, 1987).

The transect was placed perpendicular to the drainage system to minimize disturbance of the drains, which were located 15 m apart and at 1 m depth, but adjusted to the topography and natural drainage pathways (Gustafson, 1987). Wells at the site were used to collect overland flow (open circles, Fig. 1). Tile drainage discharge of the entire

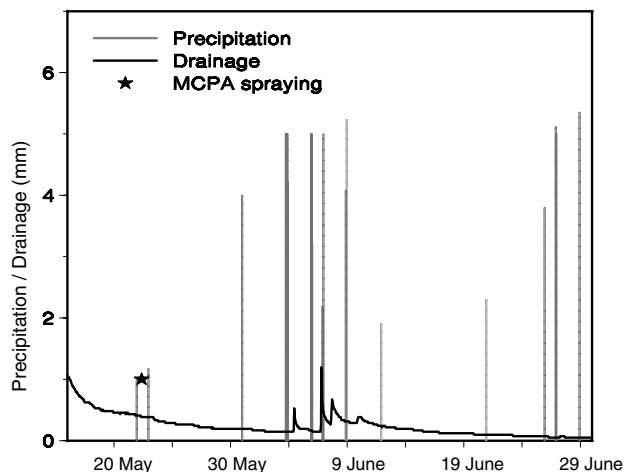


Figure 2 Hourly sums of precipitation and drainage during the simulation period 16 May–30 June. MCPA spraying occurred on 21 May 1999.

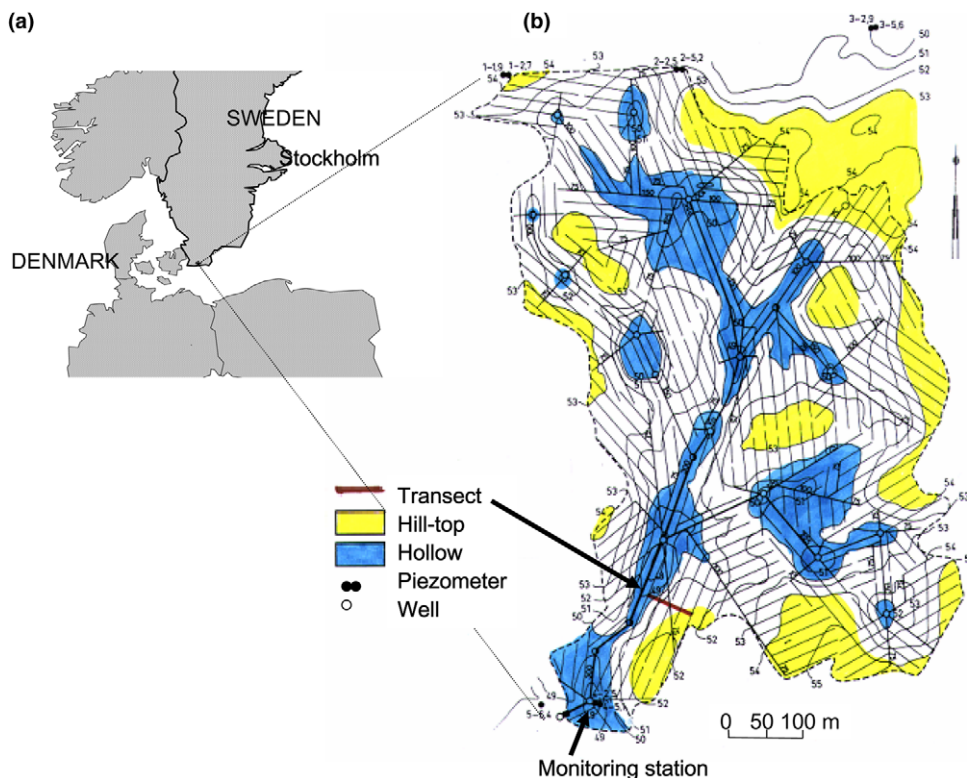


Figure 1 (a) Location of the field site within Sweden and (b) map of field site with the tile drainage system (tiles are placed at 15-m distance intervals and at 1-m depth), and positions of the transect, the tile outlet monitoring station, piezometers and wells at Näsbygård. Hilltops are shown in light grey and hollows in dark grey (source: Gustafson, 1987).

field had been monitored at the south-west corner of the field since 1973 (Fig. 1). 'Grab' water samples for pesticide analyses were taken on 13 occasions during the period May 19–June 19 1999 (Jarvis et al., 2001). The field was cropped with spring wheat (*Triticum aestivum* L.), sowed on 4 April 1999. It was conventionally tilled, with autumn ploughing and spring harrowing prior to planting. The field was sprayed with the herbicide MCPA on 21 May (40 mg m^{-2}) by the farmer using his normal equipment. Total rainfall and tile drainage amounts during the simulation period from 16 May to 30 June were 91 mm and 11 mm, respectively. After a long dry period with recessing flow, a 29 mm rain storm occurred within a few hours during the night of 3–4 June. An additional 29 mm of rain fell during the following four days, which caused peak discharges on 5–7 June 1999 (Fig. 2).

Model applications

Simulated domain, boundary and initial conditions

The simulated domain had a width of 50 m, a depth of 3 m and a height difference between the hollow and hilltop of 2.5 m (Fig. 3), since the typical length of a sequence of hilltop, mid-slope and hollow was 50 m for this field (Jarvis et al., 2001). The flow domain contained three drains at 1 m depth and 15 m apart (10, 25 and 40 m from the hollow side). The drains were simulated with the correction factor C_d and effective drain diameter d_e in Vimoke's model set to 4 and 0.04 m, respectively (Šimůnek et al., 1999).

Based on soil texture sampling, the soil profile was divided into 11 different materials (Fig. 3), with the top three layers each being 25 cm thick, and the bottom layer 2.25 m thick. The hilltop and mid-slope parts of the profiles shared the same bottom material, as well as a large part of the third layer, since the differences in texture here were insignificant (Fig. 3). The flow domain contained 23,128 unstructured triangular finite elements, with higher nodal densities in the upper 140 cm of the soil profile as well in three 1-m wide vertical columns around the drains.

The initial level of the groundwater table was set at 1 m along the hollow side, with a slope of 0.05° in the Eastern direction, based on groundwater level measurements using piezometers at four different locations in the field (Fig. 1, three piezometers along the northern border and one close to the monitoring station). The piezometric heads were recorded only once a month, which caused some uncertainty in the initial water level position since the groundwater level decreased considerably during May 1999.

Local climate conditions and root water uptake

Precipitation was recorded each day at 7 a.m. at 500 m distance from the field. Precipitation amounts measured at that time were attributed to the previous day. We assumed that all precipitation events occurred at the end of the day with a maximum rate of 5 mm per hour. Following FOCUS (2000), we assumed that 50% of the pesticide application was intercepted by the growing crop, and that 10% of the intercepted amount was washed off by each subsequent mm of rain.

Potential transpiration and evaporation were estimated with the Penman–Monteith equation (Monteith, 1965) using daily values of air temperature, radiation, wind speed, precipitation and the vapour pressure deficit (VPD) obtained from nearby meteorological stations. Radiation was partitioned between transpiration and soil evaporation according to Beer's law as a function of Leaf Area Index (LAI). Canopy resistance was estimated as a function of VPD, radiation and LAI according to the Lohammar equation (Lohammar et al., 1980; Gärdenäs and Jansson, 1995), while aerodynamic resistance above the canopy was estimated as a function of crop height and within the canopy as a function of LAI. Interception evaporation was calculated from LAI, maximum storage capacity per LAI and intercepted water (Jansson and Karlberg, 2004). Potential transpiration was corrected for interception on a daily basis. Evaporation equalled the sum of interception and soil evaporation. Parameterizations of crop characteristics and development, such as LAI (0.1–5), height (0.1–0.8 m), extinction factor for net radiation (0.5), albedo (25%) and canopy resistance were taken from Lewan (1993), Blombäck et al. (1995) and Myrbäck (1998). Soil surface resistance was set to 200 sm^{-1} (Lewan, 1993).

Root water uptake was simulated using the model of Feddes et al. (1978). The maximum rooting depth was assumed to be 1 m, with the highest root density in the upper 70 cm of soil. The critical pressure heads in the water-stress-response function of Feddes et al. (1978) were based on a study by Wesseling (1991), but adjusted for Swedish conditions according to Kätterer and Andrén (1995), leading to a value of -0.1 m for the critical wet-end pressure head h_{opt} , -15 m for the critical pressure head h_3 , and -160 m for the wilting point h_4 .

Soil hydraulic properties

Hydraulic properties of the 11 soil materials were estimated using the soil texture data from the 50-m transect and pedo-

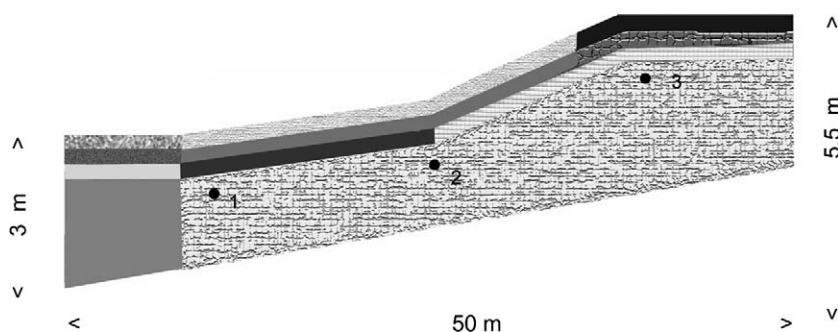


Figure 3 Simulated soil domain with the 11 different soil materials, and locations of the three drains (indicated by bold numbers).

transfer functions (see Table 2 for details) for the van Genuchten–Mualem parameters based on local data by Svensson (1999) and Jarvis et al. (2001). The saturated water content, θ_s , was estimated as a function of bulk density ρ . The bulk density and the van Genuchten shape parameter α were calculated as a function of the organic carbon content and depth, and the pore-size distribution index, n , as a function of texture, organic carbon content and depth. The pedotransfer function for the saturated hydraulic conductivity, K_s , included both porosity and the 50% water content, θ_{50} , as variables. The residual water content, θ_r , was assumed to be negligible for all materials and in all approaches, while the pore-connectivity, l , was set to 0.5 in all cases.

For the equilibrium approach, the threshold water content, θ_k , in Eq. (4) was set equal to the water content at a pressure head, h_k , of -10 cm. The hydraulic conductivity at this threshold, K_k , was set equal to the saturated matrix conductivity, K_{sm} , in the dual-permeability model, estimated with a pedotransfer function (see Tables 2 and 3).

For the dual-porosity approach, the total saturated water content, θ_s , was divided into the mobile saturated water content, θ_{sf} and the immobile saturated water content, θ_{sm} , with the assumption that the mobile water content was equal to $0.0225 \text{ m}^3 \text{ m}^{-3}$ for all soil materials (i.e. the same saturated macropore water content as for the dual-permeability approach). The water retention coefficients α_f , and n_f for the mobile zone were set to typical values for a coarse-textured soil (10 m^{-1} and 1.8, respec-

tively) so as to represent macropores; these values were assumed to be the same for all soil materials. The mass transfer coefficient, α_w , was based on calibrations carried out on 20-cm long soil columns sampled from the hollow, mid-slope and hilltop locations in the same field (Roulier and Jarvis, 2003).

For the dual-permeability approach, the ratio between total macropore and total soil volume, w , for all soil layers was set to 0.03, being the mean value estimated for soil materials 5–11 belonging to the slope and hill-top landscape elements. The macropore saturated water content, θ_{sf} , (0.75) was estimated in a similar way (multiplying w with θ_{sf} gives the same saturated macropore water content per soil volume as for the dual-porosity approach). Following Gerke and van Genuchten (1993a,b), the saturated hydraulic conductivity of the fracture–matrix interface, K_{as} , was taken to be 1% of the saturated conductivity of the matrix, the shape factor, β , was set equal to 3 (–) and the scaling factor, γ , to 0.04 (–). Values for the mass transfer coefficient, α_w , of the various layers were based on results of Roulier and Jarvis (2003).

Solute transport and reaction properties

The bulk density, ρ , the dispersion tensor, D , the first-order degradation rate constants in liquid and solid phases, μ_w and μ_s , respectively, and the transfer coefficients, α_s and ω_s , were allowed to vary with landscape position, based on studies at the same field by Jarvis et al. (2001), Roulier and Jarvis (2003), and Lindahl et al. (2005) (Table 4). The transverse dispersivity, D_T , was assumed to be 10% of the longitudinal

Table 2 Pedotransfer functions for Näsbygård (data from Jarvis et al. (2001) and Svensson (1999))

Parameter	Function	Fit and significance
Bulk density, ρ (g cm^{-3}) and porosity, ε ($\text{m}^3 \text{ m}^{-3}$)	$\rho = 1.464 + 0.05 z - 0.08 f_{oc}$ $\varepsilon = 1 - \rho / \rho_s$ $\rho_s = 2.7 - 1.7 f_{oc}$	$R^2 = 0.76, p < 0.0001$
Pore-size distribution index, n (–)	$n = \mu(0.973 - 0.345\rho) + 1$	$R^2 = 0.44, p = 0.005$
van Genuchten α_m (m^{-1})	$\text{Log } \alpha = 1.321 - 1.838\rho$	$R^2 = 0.65, p = 0.0001$
Saturated matrix water content, θ_{sm} ($\text{m}^3 \text{ m}^{-3}$)	$\theta_{10} = \theta_s^* (1 + (10\alpha)^n)^{(1/n)-1}$ $\theta_s^* = 0.96 - 0.351\rho$ $\theta_{sm} = \theta_{10} / (1 - w)$ $w = 0.03$	$R^2 = 0.84, p < 0.0001$
Saturated matrix and macropore conductivity, K_{sm} and K_{sf} (m d^{-1})	$K_{10} = 25d_g$ $\text{Log } K_s = -1.19 + 2.88 \text{ log}(100(\varepsilon - \theta_{50}))$ $\theta_{50} = \theta_s^* (1 + (50\alpha)^n)^{(1/n)-1}$ $K_{sf} = ((K_s - K_{10}) / w) \cdot (24/1000)$ $K_{sm} = (K_{10} / (1 - w)) \cdot (24/1000)$	$R^2 = 0.40, p < 0.0001$ $R^2 = 0.65, p < 0.0001$

ρ_s = particle size density (g cm^{-3}).

f_{oc} = fractional organic carbon content (–).

z = horizon number (1 = 0–25 cm, 2 = 25–50 cm, 3 = 50–75 cm, 4 = 75 + cm).

μ = particle size distribution index of van Genuchten type equation (–, based on Lindahl et al. (2005)).

θ_{10} and θ_{50} = Water content at $\psi = -10$ and -50 cm respectively ($\text{m}^3 \text{ m}^{-3}$).

θ_s^* = Saturated water content ($\text{m}^3 \text{ m}^{-3}$).

K_{10} = Hydraulic conductivity at $\psi = -10$ cm (cm h^{-1}).

d_g = characteristic particle size of van Genuchten type equation (mm, based on Lindahl et al. (2005)).

Table 3 Hydraulic parameters for the matrix (subscript m) and macropore (subscript f) regions of the different soil materials as used in the various modeling approaches: (a) equilibrium, (b) dual-porosity and (c) dual-permeability

(a) Equilibrium														
Landscape element	Soil depth (cm)	Bulk characteristics						Threshold characteristics						
		θ_r (m^3m^{-3})	θ_s (m^3m^{-3})	α (m^{-1})	n (-)	K_s (md^{-1})	l (-)	θ_k (m^3m^{-3})	K_k (md^{-1})					
Hollow	0–25	0	0.489	6.5	1.165	1.747	0.5	0.439	0.025					
	25–50	0	0.473	5.5	1.153	1.107	0.5	0.430	0.022					
	50–75	0	0.466	5.1	1.153	0.964	0.5	0.425	0.023					
	75–300	0	0.517	10.0	1.150	0.400	0.5	0.453	0.019					
Slope	0–25	0	0.475	5.5	1.149	1.056	0.5	0.433	0.025					
	25–50	0	0.442	3.7	1.134	0.411	0.5	0.410	0.024					
	50–75	0	0.417	2.7	1.128	0.209	0.5	0.391	0.025					
Slope and Hilltop	75–300	0	0.395	2.1	1.131	0.025	0.5	0.372	0.019					
Hilltop	0–25	0	0.476	5.6	1.129	0.815	0.5	0.436	0.024					
	25–50	0	0.447	3.9	1.120	0.376	0.5	0.415	0.018					
	50–75	0	0.423	2.9	1.123	0.228	0.5	0.396	0.006					
(b) Dual-porosity														
Landscape element	Soil depth (cm)	Matrix			Macropore				Transfer					
		θ_{sm} (m^3m^{-3})	α_m (m^{-1})	n_m (-)	K_{sf} (md^{-1})	θ_{sf} (m^3m^{-3})	α_f (m^{-1})	n_f (-)	α_w ($m^{-1}d^{-1}$)					
Hollow	0–25	0.464	6.5	1.165	22.288	0.0225	10	1.8	0.02					
	25–50	0.448	5.5	1.153	17.313	0.0225	10	1.8	0.02					
	50–75	0.441	5.1	1.153	16.866	0.0225	10	1.8	0.02					
	75–300	0.492	10.0	1.15	32.321	0.0225	10	1.8	0.02					
Slope	0–25	0.450	5.5	1.149	15.711	0.0225	10	1.8	0.01					
	25–50	0.417	3.7	1.134	8.142	0.0225	10	1.8	0.01					
	50–75	0.392	2.7	1.128	4.820	0.0225	10	1.8	0.01					
Slope and Hilltop	75–300	0.370	2.1	1.131	3.305	0.0225	10	1.8	0.01					
Hilltop	0–25	0.451	5.6	1.129	13.041	0.0225	10	1.8	0.001					
	25–50	0.422	3.9	1.12	7.784	0.0225	10	1.8	0.001					
	50–75	0.398	2.9	1.123	5.813	0.0225	10	1.8	0.001					
(c) Dual-permeability														
Landscape element	Soil material (cm)	Matrix				Macropore				Transfer				
		θ_{sm} (m^3m^{-3})	α_m (m^{-1})	n_m (-)	K_{sm} (md^{-1})	θ_{sf} (m^3m^{-3})	α_f (m^{-1})	n_f (-)	K_{sf} (md^{-1})	w (-)	α_w ($m^{-1}d^{-1}$)	β (-)	γ (-)	K_{sa} (md^{-1})
Hollow	0–25	0.480	6.5	1.165	0.025	0.75	10	1.8	22.288	0.03	0.01	3	0.4	0.00025
	25–50	0.480	5.5	1.153	0.022	0.75	10	1.8	17.313	0.03	0.01	3	0.4	0.00025
	50–75	0.464	5.1	1.153	0.023	0.75	10	1.8	16.866	0.03	0.01	3	0.4	0.00025
	75–300	0.457	10.0	1.150	0.019	0.75	10	1.8	32.321	0.03	0.01	3	0.4	0.00025
Slope	0–25	0.509	5.5	1.149	0.025	0.75	10	1.8	15.711	0.03	0.01	3	0.4	0.00025
	25–50	0.466	3.7	1.134	0.024	0.75	10	1.8	8.142	0.03	0.01	3	0.4	0.00025
	50–75	0.432	2.7	1.128	0.025	0.75	10	1.8	4.820	0.03	0.01	3	0.4	0.00025
Slope and Hilltop	75–300	0.406	2.1	1.131	0.019	0.75	10	1.8	3.305	0.03	0.01	3	0.4	0.00025
Hilltop	0–25	0.384	5.6	1.129	0.024	0.75	10	1.8	13.041	0.03	0.01	3	0.4	0.00025
	25–50	0.468	3.9	1.120	0.018	0.75	10	1.8	7.784	0.03	0.01	3	0.4	0.00025
	50–75	0.438	2.9	1.123	0.006	0.75	10	1.8	5.813	0.03	0.025	3	0.4	0.00025

dispersivity, D_L , consistent with limited literature data (e.g., Fetter, 1979). The fraction of the sorption sites in the macropore volume f was taken to be 1% of the total sorption sites (Roulier and Jarvis, 2003). The distribution coefficient K_d for MCPA was calculated as a function of the organic carbon content and the organic carbon partition coefficient, K_{oc} , of

$75 \text{ cm}^3 \text{ g}^{-1}$. A linear MCPA adsorption isotherm was assumed in accordance with Helweg (1987) and Riise et al. (1994). The MCPA first-order degradation rate in the solid phase, μ_s , was assumed to be equal to that in the liquid phase, μ_w .

In the mobile-immobile approach, the immobile water content, θ_{im} , was set equal to 0.15. Since θ_{im} in the

Table 4 Values of solute transport and reaction parameters of the different soil materials used in the various modeling approaches

Landscape element	Soil depth (cm)	All approaches					Dual-permeability	Mobile-immobile and dual-porosity
		ρ (kg m ⁻³)	D_L (m)	D_T (m)	K_d (l kg ⁻¹)	μ_w (d ⁻¹)	α_s (d ⁻¹)	ω_s (d ⁻¹)
Hollow	0–25	1200	0.1	0.01	1.35	0.33	0.096	0.0336
	25–50	1200	0.1	0.01	1.45	0.33	0.096	0.0336
	50–75	1200	0.1	0.01	1.75	0.33	0.096	0.0336
	75–300	1200	0.1	0.01	3.61	0.33	0.096	0.0336
Slope	0–25	1400	0.1	0.01	0.102	0.38	0.024	0.0084
	25–50	1400	0.1	0.01	0.734	0.38	0.024	0.0084
	50–75	1400	0.1	0.01	0.576	0.38	0.024	0.0084
Slope and Hilltop	75–300	1400	0.1	0.01	0.331	0.38	0.024	0.0084
Hilltop	0–25	1500	0.2	0.02	0.979	0.42	0.00176	0.000616
	25–50	1500	0.2	0.02	0.598	0.42	0.00176	0.000616
	50–75	1500	0.2	0.02	0.410	0.42	0.00176	0.000616

mobile-immobile approach is constant during the simulations, the total water content can never decrease below this value. This in contrast with the dual-porosity approach, where the immobile water content may vary with time. The maximum immobile water content in the dual porosity approach was assumed to be 0.35. The solute mass transfer coefficient of the dual-permeability approach, α_s , was estimated from the results of Roulier and Jarvis (2003). Finally, we note that the rate coefficient, ω_s , in Eqs. (14) and (15) for the mobile-immobile and dual-porosity approaches, lumps the effects of the traditional mass transfer coefficient, α_s , and the immobile (matrix) water content.

Results

Measured and simulated drainage discharge dynamics

Measured and simulated drainage rates using the different approaches are shown in Fig. 4. Notice that the vertical axis in each plot was scaled to the peak discharge rate. No separate results for the water balance of the mobile-immobile approach are given since the water balance is the same as for the equilibrium approach. Table 5 lists cumulative drainage amounts for selected periods during the experiment. Whereas the equilibrium approach simulated the correct amount of cumulative drainage for the period 3–9 June (Table 5), the largest peak in the simulated drainage flow was only one third of the measured peak rate (Fig. 4a and b). More importantly, the equilibrium approach simulated the flow peaks several days too late, thus failing to capture the preferential flow character of the drainage response.

The dual-permeability and dual-porosity approaches both simulated the timing of the first drainage flow peak fairly accurately (Fig. 4a, c and d). Simulated results showed a lag of about 10 h behind the measured data. We attribute this due to the uncertainty in the precipitation data, which had been recorded only once a day at 7 a.m.

the following morning. However, the dual-porosity and dual-permeability models both overestimated the measured peaks in the drainage rates, especially the first peak. Total cumulative drainage as calculated with the dual-porosity and dual-permeability overestimated the measurements by factors of 2.5 and 5.6, respectively (Table 5). Notice that the dual-porosity approach predicted very high peaks in the drainage outflow, but of much shorter duration, as compared to the dual-permeability approach. In the dual-porosity approach, all water flow occurs in the fast flow region (see Table 1). For the dual-permeability, some of water volume is exchanged with the matrix which reduces peak flow rates.

Better agreement between measured and simulated tile drainage rates could probably have been obtained by adjusting the soil hydraulic properties for each modelling approach separately. This was not done here in view of our aim to compare the effects of the different conceptual approaches to modelling preferential flow and transport. Separate adjustment of the soil hydraulic properties for each approach would have biased the comparisons. Instead, the hydraulic properties for the different approaches were parameterized as consistently as possible with independent measurements and available data. We found that the dual-permeability model best captured the measured dynamics in the drainage flow rate at our field site, although overestimating total tile drainage flow. Macropore flow dominated total drainage (matrix flow is the difference between total and macropore flow, see Fig. 4d), even though the macropores were estimated to comprise only 2.25% of the total soil volume.

One possible explanation for overestimation of the cumulative drainage and peak outflows is that in reality some water may have bypassed the drains to the deeper subsurface and underlying aquifer, while we used a zero-flux condition at the bottom boundary of the simulated flow domain. Although the subsoils of these clayey till soils are dense and quite impermeable, Gustafson (1987) made water balance calculations showing annual groundwater recharge

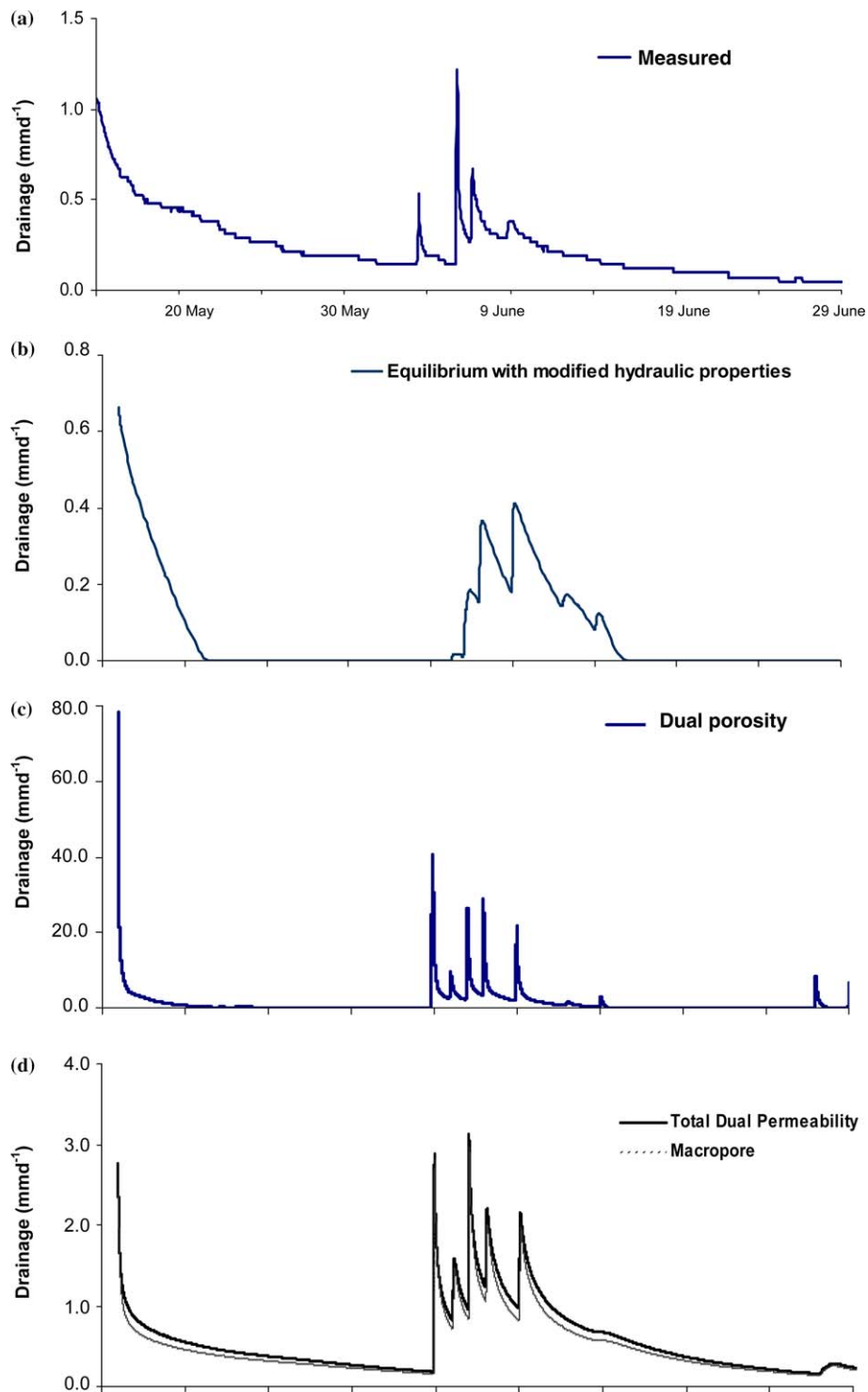


Figure 4 Measured and simulated tile drainage rates for the different approaches (a) measured, (b) equilibrium model with modified hydraulic properties, (c) dual-porosity model, and (d) dual-permeability model with total (bold solid line) and macropore flow (dashed line).

rates of between 20 and 70 mm under this field. If assumed to be constant over the year, this would have amounted to between 3 and 8 mm for the 44-day time period of our experiments, which is not enough to explain the relatively large differences in Table 5. Measurements with, some water bypassing the drains is very likely. Still, measurements with

the isotope O^{18} on samples from the piezometer closest to the drainage monitoring station (see Fig. 1 for location) indicated significant bypass of infiltrating 'new' water to shallow groundwater (Barbro Ulén, Dept. of Soil Science, SLU, Uppsala, pers. comm., 9 Feb., 2005). Another possible reason for the overestimation is uncertainty in the initial groundwa-

Approach	Cumulative drainage (mm)			
	Measured	Equilibrium, mobile–immobile	Dual-porosity	Dual-permeability
16 May–2 June	5.6	1.4	14.0	7.9
3–9 June	1.9	2.2	31.8	7.3
10–29 June	<u>2.6</u>	<u>0.1</u>	<u>11.2</u>	<u>10.2</u>
Total	10.1	3.7	57.0	25.4

ter level. We re-ran the simulations using initial groundwater levels 20 cm higher and 10 cm lower than those assumed in the earlier calculations (1 m). Initial groundwater levels at

depths of 0.8 and 1.10 m resulted in cumulative drainage rates of 39 and 19 mm, respectively, for the dual-permeability approach (as compared to 25.4 mm for the initial water

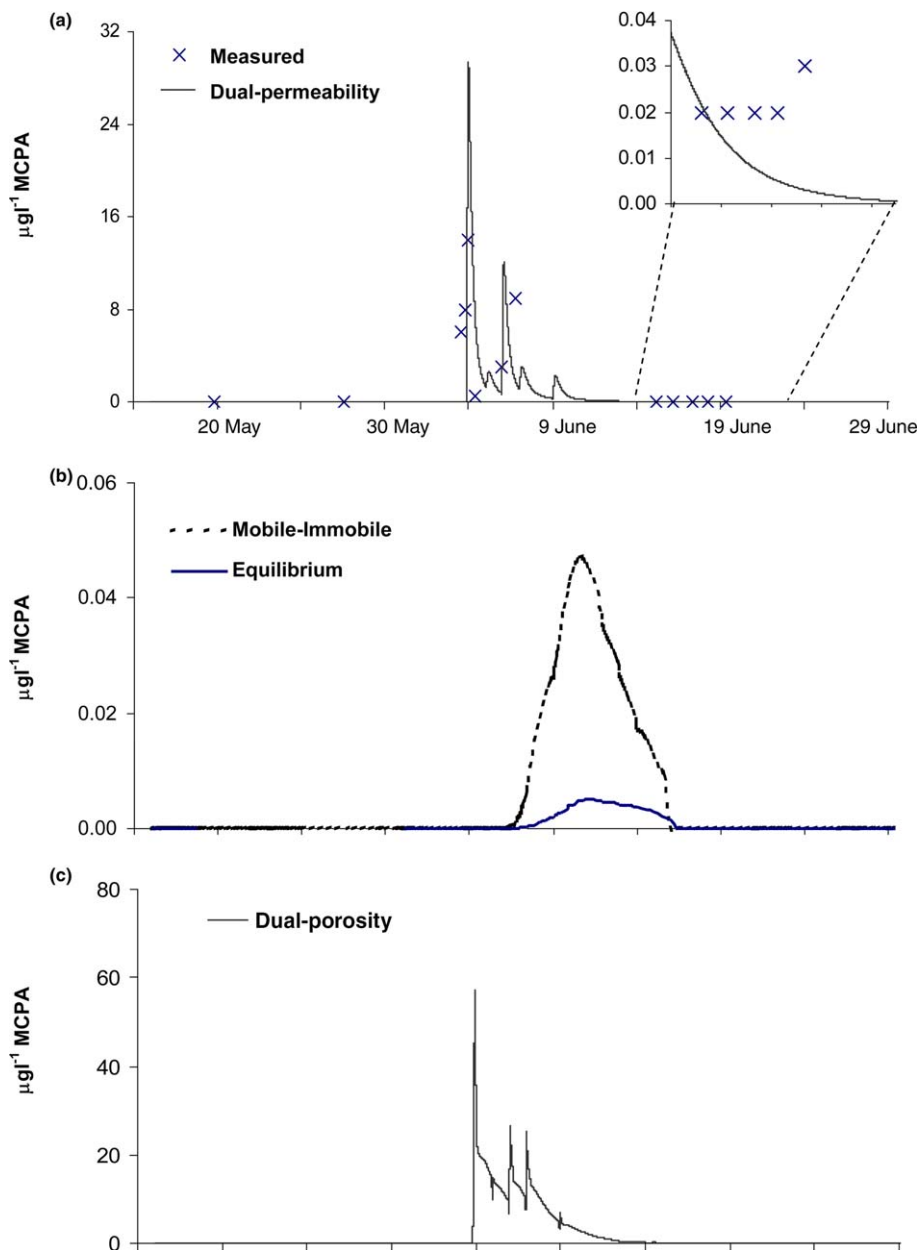


Figure 5 Measured and simulated pesticide concentrations of the drainage water for the different approaches (a) measured (crosses) and dual-permeability approach (solid line), (b) equilibrium (solid line) and mobile–immobile (dashed line) and (c) dual-porosity.

table being at 1 m, and a measured cumulative rate of 10.1 mm). Cumulative drainage hence was found to be quite sensitive to the initial groundwater level.

Measured and simulated pesticide concentrations

Pesticide concentrations (Fig. 5) in the drainage water simulated with the different approaches showed similar patterns versus time as the simulated tile drainage rates. The equilibrium and mobile–immobile approaches significantly underestimated the measured pesticide concentrations, and simulated the increase in concentrations much too late and too slow compared to the measured data. The mobile–immobile approach was able to increase the pesticide concentration by one magnitude compared to equilibrium transport, but produced only a slightly earlier appearance of the MCPA in the tile drains (Fig. 5b). By comparison, the dual-permeability and dual-porosity approaches captured the dynamics of the measured pesticide concentrations quite well. Since the automatic water sampling equipment failed and samples had to be taken manually instead, some uncertainty existed as to whether or not the events with the largest concentrations were sampled correctly. For these reasons we did not further calculate whether and by how much the simulations overestimated the measured concentrations. Irrespective of this uncertainty, Fig. 5a show very good agreement between the dual-permeability modelling results and the measured data. Results probably could have been further improved by treating the pesticide mass transfer coefficient as a calibration parameter. Similarly as for the soil hydraulic parameters, the mass transfer coefficient was taken from Roullet and Jarvis (2003).

The sampling for MCPA concentration measurements started on 19 May 1999 (i.e. two days before MCPA spraying) and continued until 19 June 1999. During periods of drainage recession it is not unusual to find traces of pesticides in the tile drainage water from earlier applications. One measurement just above the detection limit of 0.02 µg/l was made 2 days before spraying on 19 May. Another measurement on 25 May was below the detection limit, while several measurements during 15–19 June 1999 were just above the detection limit. The dual-permeability and dual-porosity models were found to simulate this pattern well (see close-up in Fig. 5a for the dual-permeability results).

Similarly as for the drainage water, we expected some overestimation of the total pesticide load in the tile drainage since groundwater recharge between the drains was neglected in the simulations. Unfortunately, the quality of pesticide data, together with the uncertainties in the water balance, did not allow us to obtain a reliable mass balance.

Discussion and conclusions

The dual-permeability approach involving two mobile flow regions most accurately simulated the measured dynamics of pesticide leaching from this undulating, tile-drained field in southern Sweden, even though it overestimated total drainage. Gerke and Köhne (2004) also found that the dual-permeability approach could capture the presumed

non-equilibrium transport processes of a field tracer experiment at a tile-drained field in Germany. An attractive feature of the dual-permeability model is the ability to simulate both the peak flow resulting from macropore flow, and the base flow reflecting matrix characteristics. The equilibrium and mobile–immobile approaches with modified hydraulic properties close to saturation failed to simulate the preferential nature of the flow process, while the dual-porosity approach assuming only mobile water in the macropore volume overestimated the degree of preferential flow.

Differences between measured and simulated tile drainage rates using the dual-permeability approach could be partly explained by water bypassing the tile drains and recharging the deeper aquifer. Better agreement between measured and simulated tile drainage rates could probably be obtained by adjusting the soil hydraulic properties for each modelling approach separately. This was not done here in view of our aim to compare the effects of the different conceptual approaches to modelling preferential flow and transport. An alternative approach for model comparison would be to allow separate parameterizations for each approach using inverse modelling (e.g., Köhne et al., 2004; Coquet et al., 2005). While this is possible at least in theory, practical problems with ill-posedness are to be expected for studies of the type considered here, involving a relatively large spatial scale with many different soil materials, as well as alternative conceptualizations and numbers of unknown parameters (see review by Šimůnek et al., 2003). The dual-permeability and dual-porosity approaches in this study captured the dynamics in measured pesticide concentrations quite well. Unfortunately, the limited number of available pesticide samples hampered accurate evaluation of the simulated pesticide concentrations, and did not permit accurate mass balance calculations. In hindsight, simultaneously collected data on conservative tracer transport would have helped us to better identify the major transport mechanisms and pathways as compared to the current study for which only flow and reactive chemical transport data were available.

Two-dimensional dual-permeability modelling for applications like the current field experiment can require considerable CPU time. The simulations in our case involved some 23,000 finite elements and 11 soil materials, requiring almost 130,000 iterations for the 1.5-month long simulation. For these reasons the use of one-dimensional models may be justified if they can capture the most important processes involved. In our case, the choice between one- and two-dimensional modelling depended very much on the possible importance of lateral flow. We knew from earlier studies that the hollows in our experimental field have relatively high organic matter contents (Jarvis et al., 2001). If transported laterally from the hilltops to the hollows, the pesticides may be adsorbed in the hollows and subsequently decomposed. We examined the importance of this lateral water flow using the dual-permeability approach. Simulations showed that the vertical component of macropore flow dominated in the vadose zone, while in the saturated zone the lateral macropore flow component was much more important. The lateral flow velocities in the macropore domain were found to be relatively constant in time during the simulations. Drain no. 3 at the boundary of the hilltop and

mid-slope area remained in the unsaturated zone during the entire simulation. Macropore flow from the hilltop area hence did not end up in the nearest tile drain, but instead moved mostly vertically into the saturated zone and then laterally to drains 1 and 2. Clearly, these lateral flow processes cannot be captured using a one-dimensional model.

Another suitable process to study with a two-dimensional model in a future project would be to evaluate the importance of the position of the drains in order to minimize leaching of agricultural chemicals. For example, shifting the drains in our study several meters towards the hollow may reduce pesticide leaching since there the flow velocities are much smaller, while the potential for pesticides sorption is much higher. We conclude that two-dimensional models are suitable tools for studying pesticide leaching from undulating fields with large spatial variability in soil properties.

Acknowledgements

We wish to acknowledge several colleagues at the Dept. of Soils Sciences, Swedish University of Agricultural Sciences: Christina Öhman for her valuable help with soil physical analyses, Erarso Etana and Laurant Brodeau for assistance in the field, and Göran Johanson and Barbro Ulén for supplying data and valuable input in the discussions. We also like to acknowledge Näsbygård (Kjell Thuresson) for giving us access to the site and supplying crop and management data. Swedish Research Council (VR, formerly NFR) supported the study financially. This study was also partly supported by the SAHRA Science Technology Center as part of NSF grant EAR-9876800, and by Carl Von Horn's Foundation and Formas through travel grants. Two anonymous reviewers are acknowledged for many useful suggestions that improved the manuscript.

References

- Abbaspour, K.C., Kohler, A., Šimůnek, J., Fritsch, M., Schulin, R., 2001. Application of a two-dimensional model to simulate flow and transport in a macroporous agricultural field with tile drains. *Eur. J. Soil Sci.* 52, 433–447.
- Akhtar, M.S., Steenhuis, T.S., Richards, B.K., McBride, M.B., 2003. Chloride and lithium transport in large arrays of undisturbed silt loam and sandy loam soil columns. *Vadose Zone J.* 2, 715–727.
- Blombäck, K., Stähli, M., Eckersten, H., 1995. Simulation of water and nitrogen flows and plant growth for a winter wheat stand in central Germany. *Ecol. Model.* 81, 157–167.
- Brown, C.D., Marshall, V., Deas, A., Carter, A.D., Arnold, D., Jones, R.L., 1999. Investigation into the effect of tillage on solute movement to drains through a heavy clay soil. II. Interpretation using a radio-scanning technique, dye tracing and modelling. *Soil Use and Management* 15, 94–100.
- Castiglione, P., Mohanty, B.P., Shouse, P.J., Šimůnek, J., van Genuchten, M.Th., Santini, A., 2003. Lateral water diffusion in an artificial macroporous system: Modeling and experimental evidence. *Vadose Zone J.* 2, 212–221.
- Christiansen, J.S., Thorsen, M., Clausen, T., Hansen, S., Refsgaard, J.C., 2004. Modelling of macropore flow and transport at catchment scale. *J. Hydrol.* 299, 136–158.
- Coquet, Y., Šimůnek, J., Coutadeur, C., van Genuchten, M.Th., Pot, V., Roger-Estrade, J., 2005. Water and solute transport in a cultivated silt loam soil: 2. Numerical analyses. *Vadose Zone J.* 4, 587–601.
- Czapar, G.F., Horton, R., Fawcett, R.S., 1992. Herbicide and tracer movement in soil columns containing an artificial macropore. *J. Environ. Qual.* 21, 110–115.
- Durner, 1994. Hydraulic conductivity estimation for soils with heterogeneous pore structure. *Water Resour. Res.* 30, 211–224.
- FAO, 1988. FAO/Unesco Soil map of the world. Revised legend. World Resources Report 60, FAO, Rome, Reprinted as Technical Paper 20, ISRIC, Wageningen, 1989.
- Feddes, R.A., Kowalik, P.J., Zaradny, H., 1978. Simulation of field water use and crop yield. *Simulation Monographs*. Centre for Agricultural Publishing and Documentation, p. 189.
- Fetter, C.W., 1979. *Contaminant Hydrology*. MacMillan Publ. Co., New York.
- Fipps, G., Skaggs, R.W., Nieber, J.L., 1986. Drains as a boundary condition in finite elements. *Water Resour. Res.* 22, 1613–1621.
- Flury, M., 1996. Experimental evidence of transport of pesticides through field soils – a review. *J. Environ. Qual.* 25, 25–45.
- FOCUS, 2000. "FOCUS groundwater scenarios in the EU review of active substances" Report of the FOCUS Groundwater Scenarios Workgroup, EC Document Reference SANCO/321/2000 rev. 2, p. 202.
- Gärdenäs, A., Jansson, P.-E., 1995. Simulated water balance of Scots Pine stands in Sweden for different climate change scenarios. *J. Hydrol.* 166, 107–125.
- Gerke, H.H., van Genuchten, M.T., 1993a. A dual-porosity model for simulating the preferential movement of water and solutes in structured porous media. *Water Resour. Res.* 29, 305–319.
- Gerke, H.H., van Genuchten, M.T., 1993b. Evaluation of a first-order water transfer term for variably saturated dual-porosity flow models. *Water Resour. Res.* 29, 1225–1238.
- Gerke, H.H., van Genuchten, M.Th., 1996. Macroscopic representation of structural geometry for simulating water and solute movement in dual-porosity media. *Adv. Water Resour.* 19, 343–357.
- Gerke, H.H., Köhne, J.M., 2004. Dual-permeability modeling of preferential bromide leaching from a tile-drained glacial till agricultural field. *J. Hydrol.* 289, 239–257.
- Gustafson, A., 1987. Simulation of water discharge rates from a clay-till soil over a ten year period. *J. Hydrol.* 92, 263–274.
- Helweg, A., 1987. Degradation and adsorption of ¹⁴C-MCPA in soil – Influence of concentration, temperature and moisture content on degradation. *Weed Res.* 27, 287–296.
- Jansson, P.-E., Karlberg, L., 2004. Coupled heat and mass transfer model for soil–plant–atmosphere systems. TRITA-LWR Report 3087, p. 427.
- Jarvis, N.J., 2002. Macropore and preferential flow. In: Plimmer, J. (Ed.), *The Encyclopedia of Agrochemicals*, vol. 3. J. Wiley and Sons, Inc., pp. 1005–1013.
- Jarvis, N.J., Stähli, M., Bergström, L., Johnsson, H., 1994. Simulation of dichlorprop and bentazon leaching in soils of contrasting texture using the MACRO model. *J. Env. Sci. Health A29*, 1255–1277.
- Jarvis, N., Gärdenäs, A., Alavi, G., Kreuger, J., 2001. In: Holman, I., Hollis, J. (Eds.), *CAMSCALE: upscaling, predictive models and catchment water quality*. Final Report ENV4-CT97-0439, Soil Survey and Land Research Centre, Silsoe, United Kingdom. pp. 12–18.
- Kamra, S.K., Lennartz, B., van Genuchten, M.Th., Widmoser, P., 2001. Evaluating non-equilibrium solute transport in small columns. *J. Contam. Hydrol.* 48, 189–212.
- Kätterer, T., André, O., 1995. Measurements and simulations of heat and water balance components in a clay soil cropped with winter wheat under drought stress or daily irrigation and fertilization. *Irrig. Sci.* 16, 65–73.
- Kohler, A., Abbaspour, K.C., Fritsch, M., van Genuchten, M.Th., Schulin, R., 2001. Simulating unsaturated flow and transport in a

- macroporous soil to tile drains subject to an entrance head: model development and preliminary evaluation. *J. Hydrol.* 254, 67–81.
- Kohler, A., Abbaspour, K.C., Fritsch, M., Schulin, R., 2003. Using simple bucket models to analyze solute transport to subsurface drains by preferential flow. *Vadose Zone J.* 2, 68–75.
- Köhne, J.M., Köhne, S., Mohanty, B.P., Šimůnek, J., 2004. Inverse mobile–immobile modeling of transport during transient flow: Effects of between-domain transfer and initial water content. *Vadose Zone J.* 3, 1309–1321.
- Köhne, J.M., Gerke, H.H., 2005. Spatial and temporal dynamics of preferential bromide movement towards a tile drain. *Vadose Zone J.* 4, 79–88.
- Larsbo, M., Jarvis, N., 2003. MACRO 5.0. A model of water flow and solute transport in macroporous soil. Technical description. Emergo 2003:6. Swedish. Univ. of Agric. Sci., Dept. of Soil Sci, Div. of Env. Phys. ISBN 91-576-6592-3.
- Lennartz, B., 1999. Variation of herbicide transport parameters within a single field and its relation to water flux and soil properties. *Geoderma* 91, 327–345.
- Lewan, E., 1993. Evaporation and discharge from arable land with cropped or bare soils during winter. Measurements and simulations. *Agric. Forest Meteorol.* 64, 131–159.
- Liljequist, G.H., 1970. Climatology. Generalstabens Litografiska Anstalt, Stockholm, p. 427. (In Swedish).
- Lindahl, A., Kreuger, J., Stenström, J., Gärdenäs, A., Alavi, G., Roulier, S., Jarvis, N., 2005. Stochastic modelling of diffuse pesticide losses from a small agricultural catchment. *J. Environ. Qual.* 34, 1174–1185.
- Ljung, G., 1987. Mekanisk analys. Beskrivning av en rationell metod för jordartsbestämning. *Swed. Univ. of Agric. Sci., Dept. of Soil Sci., Div. Agric. Hydrotechnics, Communication* 87:2, p. 9 (In Swedish).
- Lohammar, T., Larsson, S., Linder, S., Falk, S.O., 1980. FAST – simulation models of gaseous exchange in Scots pine. In Persson, T. (Ed.), *Structure and Function of Northern Coniferous Forests – An Ecosystem Study*, Stockholm, *Ecol. Bull.* vol. 32, pp. 505–523.
- Mohanty, B.P., Bowman, R.S., Hendrickx, J.M.H., van Genuchten, M.Th., 1997. New piecewise-continuous hydraulic functions for modeling preferential flow in an intermittent flood-irrigated field. *Water Resour. Res.* 33, 2049–2063.
- Monteith, J.L., 1965. Evaporation and environment. In: Fogg, G.E. (Ed.), *The State and Movement of Water in Living Organisms*, 19th Symp. Soc. Exp. Biol., Cambridge, The Company of Biologists, pp. 205–234.
- Myrbäck, Å., 1998. Swedish agricultural and horticultural crops. Swedish National Chemical Inspectorate PM 1/98. p. 44.
- Pot, V., Šimůnek, J., Benoit, P., Coquet, Y., Yra, A., Martínez-Cordón, M.-J., 2005. Impact of rainfall intensity on the transport of two herbicides in undisturbed grassed filter strip soil cores. *J. of Contaminant Hydrology* 81, 63–88.
- Riise, G., Eklo, O.M., Pettersen, M.N., Salbu, B., 1994. Association of MCPA, dichlorprop, tribenuron-methyl, atrazine and dimethoate with different soil types – Laboratory experiments. *Norw. J. Agric. Sci.* 13 (supplement), 17–29.
- Roulier, S., Jarvis, N., 2003. Modeling Macropore Flow Effects on Pesticide Leaching: Inverse Parameter Estimation using Micro-Lysimeters. *J. Environ. Qual.* 32, 2341–2353.
- Saxena, R.K., Jarvis, N.J., Bergström, L., 1994. Interpreting non-steady state tracer breakthrough experiments in sand and clay soils using a dual-porosity model. *J. Hydrol.* 162, 279–298.
- Šimůnek, J., Šejna, M., van Genuchten, M.Th., 1999. The HYDRUS-2D software package for simulating two-dimensional movement of water, heat, and multiple solutes in variably saturated media. Version 2.0, IGWMC – TPS – 53, International Ground Water Modeling Center, Colorado School of Mines, Golden, Colorado, p. 251.
- Šimůnek, J., Jarvis, N.J., van Genuchten, M.Th., Gärdenäs, A., 2003. Review and comparison of models for describing non-equilibrium and preferential flow and transport in the vadose zone. *J. Hydrol.* 272, 14–35.
- Stamm, C., 1997. Rapid transport of phosphorus in drained grasslands soils. PhD Dissertation No. 12486, Swiss Federal Institute of Technology, Zürich.
- Svensson, O., 1999. Markkaraktärisering av ett avrinningsområde i södra Skåne. Division of Water Quality Management, Swedish University of Agricultural Sciences, Uppsala, Sweden. Seminars and MSc thesis no. 31, p. 15. (in Swedish with English abstract).
- van Genuchten, M.Th., 1980. A closed-form equation for predicting the hydraulic conductivity of unsaturated soils. *Soil Sci. Soc. Am. J.* 44, 892–898.
- van Genuchten, M.Th., Wierenga, P.J., 1976. Mass transfer studies in sorbing porous media, I. Analytical solutions. *Soil Sci. Soc. Am. J.* 40, 473–481.
- Vimoke, B.S., Tura, T.D., Thiel, T.J., Taylor, G.S., 1963. Improvements in construction and use of resistance networks for studying drainage problems. *Soil Sci. Soc. Am. Proc.* 26 (2), 203–207.
- Vogel, T., Císlarová, M., 1988. On the reliability of unsaturated hydraulic conductivity calculated from the moisture retention curve. *Transp. Porous Media* 3, 1–15.
- Wesseling, J.G., 1991. Meerjarige simulaties van grondwateronttrekking voor verschillende bodemprofielen, grondwatertrappen en gewassen met het model SWATRE, Report 152, Winand Staring Centre, Wageningen (In Dutch).